

KAWASAKI STEEL TECHNICAL REPORT

No.30 (August 1994)

Special Issue on LSI

Improvement of Electromigration Resistance of AlCu/TiN Lines by Controlling Aluminum Microstructure

Takenao Nemoto, Hiroshi Horikoshi, Takeshi Nogami

Synopsis :

Two techniques for improving electromigration (EM) resistance of AlCu/TiN lines were developed by controlling the microstructure of aluminum alloys. One is control of Cu atom distribution in AlCu films by aging at 250°C for 10 h after the wafer process. Cu atom segregation to grain boundaries after aging was observed indicating importance of segregated Cu for EM resistance. The other is control of crystalline orientation of Al in AlCu/TiN lines. Deterioration of crystalline orientation was found in metallization process to form tungsten-plug contact/via. Removal of sulfur/fluorine atoms from the TiN surface on which AlCu films are to be deposited prevented the deterioration.

(c)JFE Steel Corporation, 2003

The body can be viewed from the next page.

Improvement of Electromigration Resistance of AlCu/TiN Lines by Controlling Aluminum Microstructure*



Takenao Nemoto
LSI Research Center,
High-Technology Res.
Labs.,



Hiroshi Horikoshi
Process Development
Sec., Technology
Development Center,
LSI Div.



Takeshi Nogami
Dr. Eng., Senior Re-
searcher, LSI Research
Center, High-
Technology Res. Labs.,

Synopsis:

Two techniques for improving electromigration (EM) resistance of AlCu/TiN lines were developed by controlling the microstructure of aluminum alloys. One is control of Cu atom distribution in AlCu films by aging at 250°C for 10 h after the wafer process. Cu atom segregation to grain boundaries after aging was observed indicating importance of segregated Cu for EM resistance. The other is control of crystalline orientation of Al in AlCu/TiN lines. Deterioration of crystalline orientation was found in metallization process to form tungsten-plug contact/via. Removal of sulfur/fluorine atoms from the TiN surface on which AlCu films are to be deposited prevented the deterioration.

1 Introduction

AlCu lines stacked with refractory metals have a sufficient margin in their electromigration (EM) lifetime for 0.8 μm design rule LSI devices. The margin is steeply decreased, however, as shrinkage of the design rule proceeds because of the inverse square dependence of the lifetime on the current density. Although new metallization systems such as copper interconnects¹⁾ and single crystal aluminum interconnects²⁾ are attracting increasing interest, history tells us that extending the applicability of an existing technology to finer design rules is usually more economical in both development and production than introducing a new technology. This work aims at improving EM lifetime and, as a result, extending to the sub-half-micron era, the applicability of today's most popular metallization system, TiN/AlCu/TiN/Ti multilayered lines and tungsten (W)-plug contact/via.

The reliability of this popular metallization system should be improved by controlling the microstructural features of the AlCu layer of the metal lines listed in Fig. 1. Two features of the microstructure, namely, crystalline orientation and Cu distribution, were individually controlled in this study: the former, by surface treatment of the TiN/Ti layer,^{3,4)} and the latter, by aging treatment.^{5,6)} These two techniques will be discussed in this order.

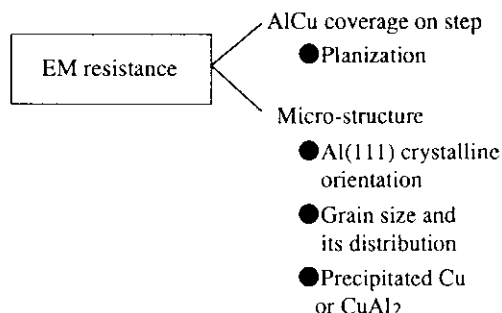


Fig. 1 Factors influencing EM resistance

2 Controlling Crystalline Orientation of AlCu Layers

2.1 Background

It is well known that the reliability of Al lines strongly correlates with their crystalline orientation and grain size.⁷⁾ Al films strongly aligned to the (111) crystalline orientation and consisting of large grains show superior EM resistance. In a modern metallization process using W-plugs to fill contact/via holes, blanket-W films deposited by CVD are etched back to form W-plugs in the holes. During etching back, a TiN film is left beneath the W film. That is, the etching back is stopped on the TiN film with some over-etching period. The remaining TiN film is then used as a part of the

* Originally published in *Kawasaki Steel Giho*, 26(1994)2, 65-70

TiN/AlCu/TiN/Ti metal line. It was supposed that during this over-etching period, the surface of the TiN film would suffer some etching damage. On the other hand, it has been reported that AlCu films sputtered on the TiN/Ti film show excellent crystalline alignment.⁸⁾ This is due to epitaxial growth of the AlCu film to the underlying TiN film, which occurs owing to a small difference in lattice constant between Al and TiN (less than 1%). Taking this epitaxial phenomenon into account, it was supposed that AlCu films sputtered onto the damaged TiN surface would grow non-epitaxially and, as a result, show poor crystalline alignment. In this study, the effects of the over-etching damage on the crystalline alignment and EM resistance of the lines were examined. After the observation of the damage effects, processes to remove the damage were investigated.

2.2 Experimental Procedure

2.2.1 Sample preparation

Three kinds of TiN/Ti layers were prepared for AlCu film deposition. TiN(100 nm)/Ti(50 nm) stacked films were deposited by DC magnetron sputtering on BPSG films on Si substrates. The first kind of TiN/Ti layers, called the sp-TiN/Ti layer, is an as-sputtered layer. The second of the TiN/Ti layers, called the eb-TiN/Ti layer, is damaged by W-etching-back process. The process flow for preparing this kind of sample is shown in Fig. 2. In this process, 1 000 nm thick blanket-W films were deposited by CVD on the TiN/Ti films and were plasma etched using a mixed gas of SF₆ and Ar. The etching was stopped on the surface of the TiN with some over-etching period. The third TiN/Ti layer is called the treated layer. Samples with eb-TiN/Ti surfaces were subjected to one of three kinds of surface treatment: (a) Ar ion sputtering, (b) wet cleaning using an ammonium hydrogen peroxide mixture (APM), and (c) wet cleaning using an organic solution.

Onto these three kinds of TiN/Ti layers, 800 nm AlCu(0.5wt.%) films were sputtered. For an EM test structure, 25 nm thick TiN films were sputtered onto the AlCu/TiN/Ti layers, resulting in a TiN/AlCu/TiN/

Ti multilayered structure. These multilayered films were patterned to metal lines with a width of 1.2 μm and length of 6 mm through conventional photolithography and dry-etching processes. These metal lines were passivated with SiN/PSG films. After annealed at 400°C for 30 min in an N₂ gas, the Si wafers were diced and the chips were assembled in a 24 DIP ceramic package.

2.2.2 Analysis

The crystalline alignment of the Al films was analyzed by X-ray diffraction (XRD). Impurities at the surface of the TiN were detected by Auger electron spectroscopy (AES). The roughness of the TiN surfaces was measured by atomic force microscopy (AFM).

2.2.3 EM test

These test structures were stressed under a current density of 4×10^6 A/cm² at 170°C. Time to failure (TTF) was defined as the time for a line to open completely, and was Weibull-plotted.

2.2 Results and Discussion

Figures 3 (a) and (b) show the rocking curve profiles of Al (111) as observed by XRD for AlCu films sputtered onto the sp-TiN/Ti and eb-TiN/Ti layers, respectively. The Al (111) intensity of the AlCu film sputtered on eb-TiN/Ti layer was one third of that for the film sputtered on sp-TiN/Ti, whereas the half width of the rocking curves for the AlCu on the eb-TiN/Ti layers was three times that with the sp-TiN/Ti layers. Both results clearly indicate a much worse (111) crystalline alignment of the AlCu film formed on the eb-TiN/Ti layers. Figure 4 shows the Weibull plot of TTFs for metal lines of the TiN/AlCu/sp-TiN/Ti and the TiN/AlCu/eb-TiN/Ti multilayers. The mean time to failure (MTF) for the lines of the eb-TiN/Ti layers was one order of magnitude smaller than that for lines of the sp-TiN/Ti layers in this figure. The fact that EM lifetime for the lines of the eb-TiN/Ti layers was about one tenth that with sp-TiN/Ti layers is in good accordance with the inferior Al (111) crystalline orientation of the AlCu on the eb-TiN/Ti layer in Fig. 3 (b).

Figure 5 (a) and (b) show AES spectra for the sp-

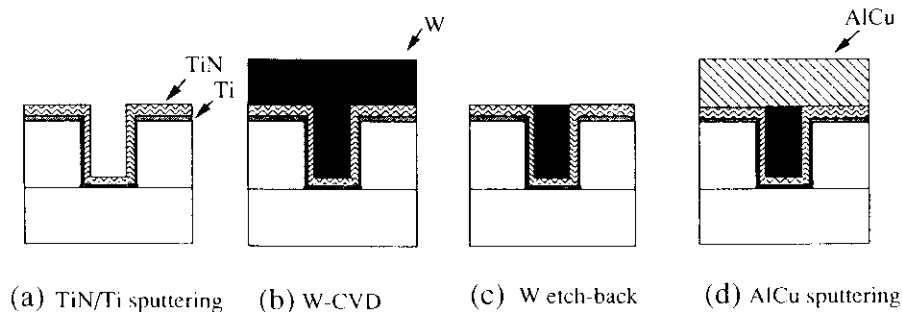


Fig. 2 Process flow preparing AlCu/TiN lines with W-CVD filling contact

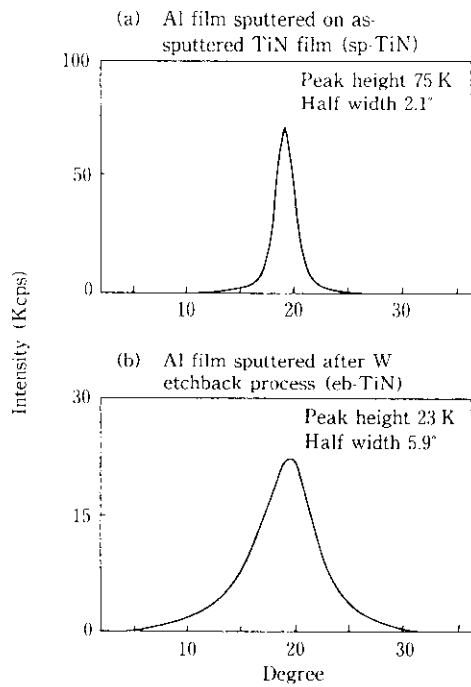


Fig. 3 Al (111) rocking curve profiles

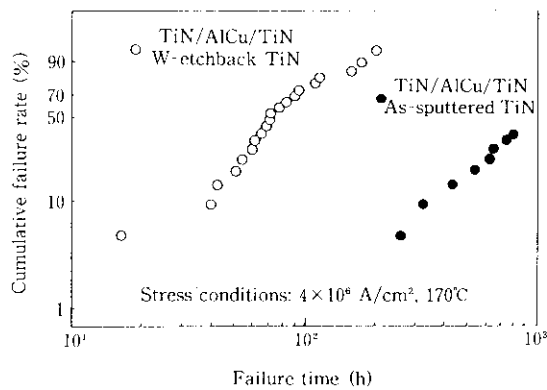


Fig. 4 Comparison of EM failure time distribution between the TiN/AlCu/eb-TiN and TiN/AlCu/sp-TiN lines

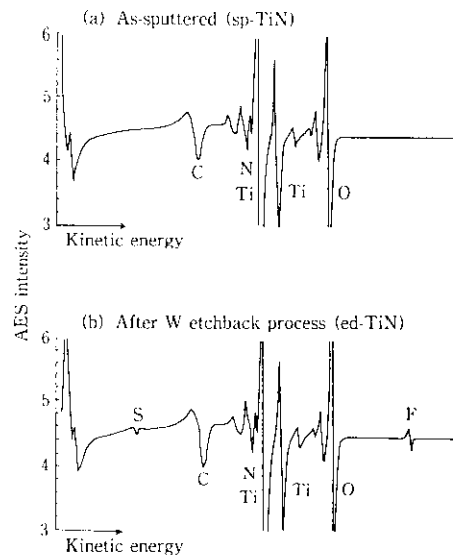
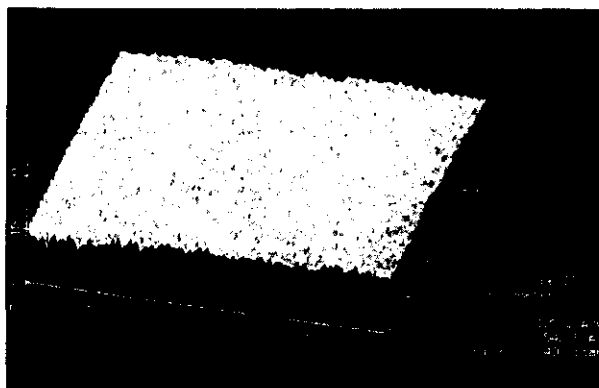


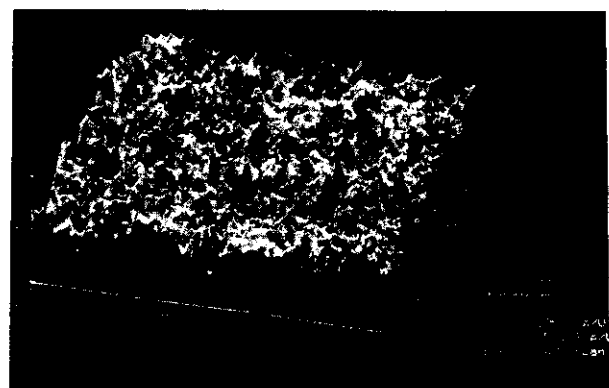
Fig. 5 AES profiles of TiN surface

TiN/Ti and eb-TiN/Ti layers, respectively. **Photo 1** (a) and (b) show AFM images for the TiN surfaces of the sp-TiN/Ti and the eb-TiN/Ti layers, respectively. In Fig. 5 (b), sulfur (S) and fluorine (F) signals were detected. In Photo 1 (b), an increase of about three times in surface roughness was observed with the eb-TiN surface. The inferior Al (111) alignment in Fig. 3 (b) is attributed to surface properties of the TiN/Ti, such as the presence of S and F atoms in Fig. 5 (b) and the increased surface roughness in Photo 1 (b).

Table 1 shows the Al (111) intensity of AlCu films sputtered onto the surfaces treated by methods (A) to (C), and the AES and AFM results for the treated TiN/Ti. As is shown in this table, the Al (111) crystalline alignment of the AlCu films sputtered on the (A) Ar ion-sputtering treated TiN/Ti and (B) APM-cleaning treated TiN/Ti was as good as that for the AlCu on the



(a) As-sputtered (sp-TiN)



(b) After W etchback process (eb-TiN)

Photo 1 AFM images of TiN surface

Table 1 TiN surface treatments and their effects on the TiN surface conditions and the crystalline orientation

Sample	Al (111) crystalline orientation	S, F on TiN surface	Roughness
(A) Ar ion sputtering	110 Kcps	non	rough
(B) Ammonium hydrogen peroxide wet treatment	125 Kcps	non	smooth
(C) Organic wet treatment	15 Kcps	present	rough
(D) W-etchback damaged TiN	23 Kcps	present	rough

sp-TiN/Ti layers in Fig. 2 (a). A cause for deterioration in Al (111) alignment on the eb-TiN surface can thus be removed by the two treatments, (A) and (B). Neither S and F was observed on the (A) treated and (B) treated TiN surface, while both were observed on the (C) treated TiN surface. On the hand, while the (B) or (C) treated TiN surfaces have almost the same roughness as the eb-TiN surface, the (A) treated TiN surface has a larger roughness than the others.

The cause to be removed by the two kinds of surface treatments, (A) and (B) in Table 1, appears to be strongly related to the presence of S and F atoms rather than increased surface roughness, because the epitaxial growth of (111) oriented Al films on the (111) oriented TiN films is thought to be disturbed by the presence of compounds such as TiF_4 and TiS_2 on the TiN surface.

3 Controlling Cu Atom Distribution

3.1 Background

It is well known that Al lines containing Cu have a high EM resistance and these are now widely used. The most popularly used Al line is alloyed with 0.5wt.% Cu.⁹⁾ It is not clear whether higher contents of Cu than 0.5wt.% would bring about further improvement of EM resistance. However, it should be noted that Al alloys are susceptible to corrosion when Cu is added. A rather low content of Cu, 0.5wt.%, has been used taking corrosion into account, and a trial to extend today's metal system to an era of reduced design rules using AlCu films with higher Cu contents is not recommended. Rather, it is important to optimize the Cu atom distribution in Al alloys by understanding how the Cu atoms improve EM resistance.

In this study, low-temperature annealing at 250°C for 10 to 100 h was applied to the AlCu/TiN multilayered lines after all wafer processes were complete in order to redistribute the Cu atoms. Here the term "aging treatment" is used to describe such low-temperature annealing.

3.2 Aging Treatment and Expected Effect

The normal temperature range of wafer processing after AlCu sputtering (CVD, 350-400°C) is indicated by

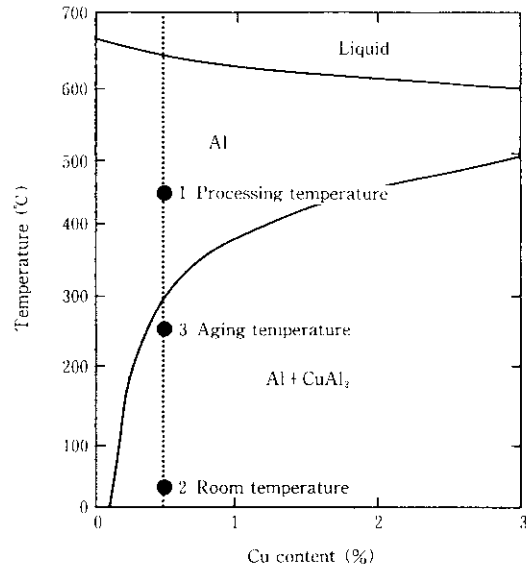


Fig. 6 Al-Cu phase diagram¹⁵⁾

1 on the Al-Cu phase diagram¹⁰⁾ in Fig. 6. This figure shows that, during wafer processing, little $CuAl_2$ will precipitate in the Al films.

It can also be predicted from this figure that sufficiently slow cooling from the process temperature to room temperature (indicated by 2 in Fig. 6) will promote $CuAl_2$ precipitation. However, the diffusion length of Cu during cooling, calculated using the diffusion coefficient of Cu in Al¹¹⁾ was only 0.2-0.5 μm , which is far smaller than the 2.0 μm average grain size observed by TEM. Therefore, Cu atoms will not diffuse in grains during cooling in adequate numbers to form precipitates at the grain boundaries, due to the low diffusivity of Cu. In other words, the Cu atoms in AlCu(0.5wt.%) lines just after processing are supersaturated.

Additional heating for a long period after processing will promote Cu diffusion and precipitation at grain boundaries. The time necessary for Cu to diffuse for 1 μm at 250°C (indicated by 3 in Fig. 6) was estimated to be 10 h using the diffusivity values.¹¹⁾

From the estimated diffusion length and solid solubility of Cu, we devised and performed aging treatments

of 10, 50 and 100 h at 250°C, assuming that, in addition to Cu redistribution, such EM factors as Al grain size and Al (111) crystal orientation may also be affected by aging treatment. Therefore, measurements of these quantities were made.

3.3 Experimental Procedure

3.3.1 Sample preparation

Films of Al-0.5wt.%Cu 800 nm thick were DC-magnetron-sputtered in Ar gas on 1.0 μm thick BPSG films coating the (100) Si substrates, with the substrate at 180°C. Annealing was performed at 400°C for 30 min. The wafers were then subjected to aging treatment at 250°C for 10–100 h. These samples were prepared for analysis of the film properties.

The TiN(25 nm)/AlCu(800 nm)/TiN(100 nm)/Ti(50 nm) multilayer was sputtered on BPSG coated Si substrates to form EM test structures. These films were patterned to 1.2 μm -wide and 2.5 mm-long lines by standard photolithography and plasma dry etching. After being passivated with a SiN/PSG film, each test structure was annealed at 400°C for 30 min before aging to initialize the distribution of Cu atoms to be same as that of the films for analysis of the film properties. Then, after the structures were assembled in a ceramic package, the aging treatments were carried out under the aforementioned conditions.

3.3.2 EM test

The AlCu multilayered lines were stressed at a DC constant current of $7 \times 10^6 \text{ A/cm}^2$ at an ambient temperature of 25°C. The temperature of the Joule-heated lines during testing was estimated from the line resistivity to be 250°C.

3.3.3 AlCu film characterization

The properties of AlCu films before and after aging treatment were characterized using the following tools:

- (1) TEM to observe the microstructure of the films and the configuration of precipitates, and to measure grain size, using a Hitachi HF-2000 equipped with a field emission (FE) electron source,
- (2) EDX to detect Cu atoms inside grain, at grain boundaries and in the precipitates, focusing an electron probe to 1 nm in diameter, which was enabled by FE-TEM,
- (3) ED (electron diffraction) to analyze the lattice structure of precipitates, and
- (4) XRD to analyze Al crystalline orientation.

3.4 Results

Figure 7 shows the Weibull distribution of EM failure times for the aged and non-aged AlCu multilayered lines. As is shown in this figure, EM failure time was increased by aging treatment and varied with aging time. The MTFs in Fig. 7 are normalized by those for

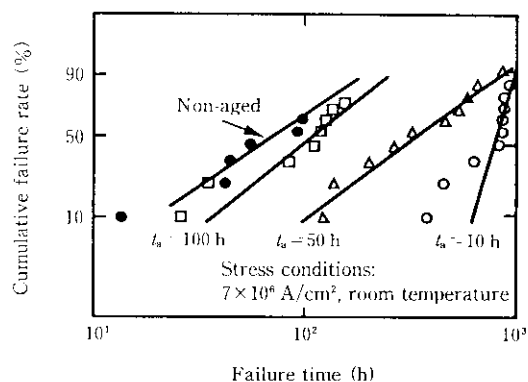


Fig. 7 EM failure time distribution for the nonaged and the aged lines for variable time

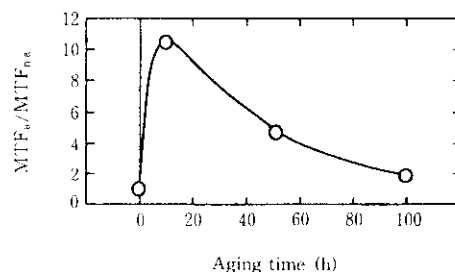


Fig. 8 MTF ratio of the aged-lines to non-aged as a function of the aged time

the non-aged lines and are plotted as a function of aging time (t_a), in Fig. 8. Failure time showed a maximum ($10\times$) at 10 h and decreased with increasing aging time.

Photo 2 (a), (b) and (c) show TEM photos of the non-aged, 10-h-aged and 100-h-aged AlCu films, respectively. Precipitates at grain boundaries, which were rarely observed in the non-aged film, were frequently observed for the aged films. These precipitates were determined to be CuAl_2 by ED analysis of their lattice constant.

Photo 3 shows an example of a TEM map of an AlCu film with detection points for EDX. The signals were detected at sites inside a grain (indicated as 1, 2, 3 in Photo 3), at grain boundaries (4, 5, 6, 7, 10) and at grain boundary triple points (8, 9, 11) for each sample with different aging times. Strong EDX intensities of Cu were detected from CuAl_2 precipitates visible by TEM (10, 11 in Photo 3) at 10 000 \times magnification. Cu intensities significantly larger than those from sites inside a grain (1, 2, 3) were also detected at grain boundaries (4, 5, 6, 7) where no precipitate was observed. The intensity varied depending on the angle of the grain boundary to the electron probe. The more perpendicular the grain boundary was to the TEM sample surface, the stronger the signal intensity was. Figure 9 shows plots of Cu intensity ratio r , as a function of aging time, where

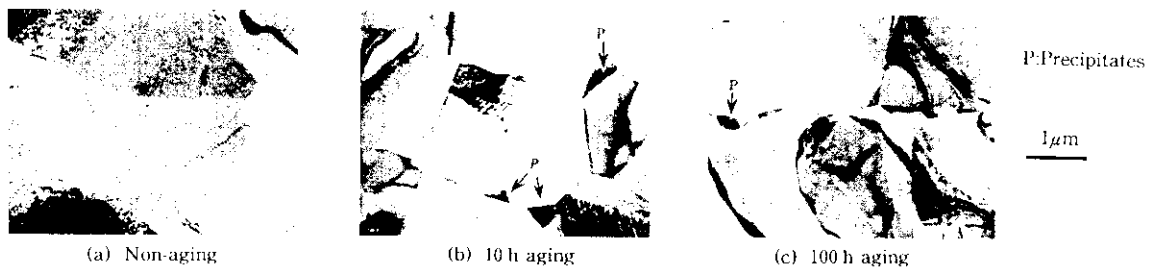


Photo 2 TEM observations of the aged and the non-aged AlCu



Photo 3 An example of EDX measuring points

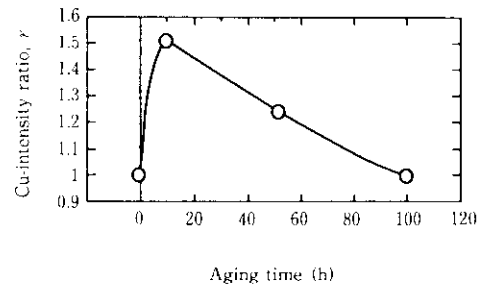


Fig. 9 EDX intensity ratio of Cu atoms at grain boundaries to inside grain as a function of the aging time

$$r = I(\text{G.B.})/I(\text{I.G.}) \quad \dots \dots \dots (1)$$

$I(\text{G.B.})$ is an average Cu intensity from grain boundaries where there is no visible precipitate and $I(\text{I.G.})$ is an average Cu intensity from sites inside grains. As is shown in Fig. 9, r increases with aging time to a maximum at 10 h and then decreases with longer times (50–100 h).

There was little difference in grain size and its variation σ observed by TEM and Al (111) crystal orientation observed by XRD between the non-aged and the aged AlCu films.

3.5 Discussion

The temporal variation of EM failure time (Fig. 8) shows the same pattern as the variation in segregated

Cu at grain boundaries detected by EDX (Fig. 9). Therefore, it was concluded that the improvement in EM resistance after aging treatment is due to the segregation of Cu at grain boundaries.

Figure 9 shows that grains after the 10 h aging treatment are coated most effectively by segregated Cu. Under these conditions, the EM lifetime is also maximum. Therefore, the microstructure in which grains are coated with Cu is the most effective for improving EM resistance. This observation is in good agreement with the results predicted by Frear et al.¹²⁾

Further aging treatment reduces the content of segregated Cu. Cu atoms diffuse toward CuAl_2 precipitates and grow into them during over-aging. A model for Cu atom redistribution during aging treatment is illustrated in Fig. 10.

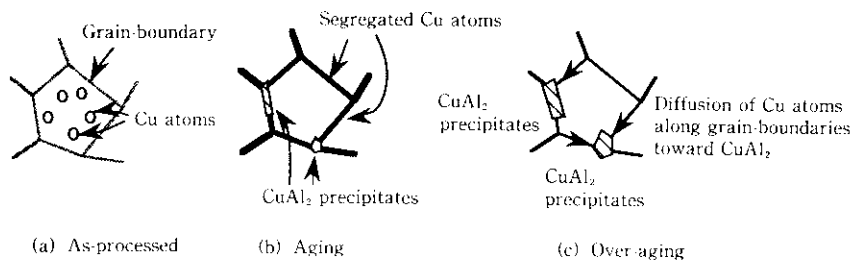


Fig. 10 Schematic of the aging mechanism

A model which explains our results has been proposed by Rosenberg et al.¹³⁾ According to this model, grain boundaries with Cu-Al bonds are more resistive to Al atom diffusion along the boundaries than those without Cu-Al bonds, because the number of vacancies in the grain boundaries is reduced by the presence of Cu atoms. The model shows how the segregated Cu atoms at grain boundaries arrested the EM of Al atoms in this work.

4 Summary

Two techniques for control of the microstructure of AlCu layers in TiN/AlCu/TiN/Ti multilayered lines have been proposed. The results are as follows:

- (1) AlCu/TiN multilayered lines formed through a W-CVD and etching back process for W-plug formation showed one order of magnitude shorter EM lifetime than those without the W-plug process. This poorer EM resistance was attributed to the inferior Al (111) crystalline alignment of AlCu films sputtered on the overetching damaged TiN/Ti layers. The presence of sulfur and fluorine were observed on the damaged TiN surface by AES.
- (2) Removal of these S and F atoms were observed with TiN surface which were sputtered by Ar ions or cleaned using the APM. AlCu films sputtered on the TiN films which were treated by one of these two treatments showed Al (111) alignment as good as that of the non-damaged TiN/Ti layer. Therefore, a cause of deterioration in Al (111) alignment is strongly related to the presence of S and F atoms on the overetching damaged TiN surface. Specifically, epitaxial growth of (111) oriented Al films on (111) oriented TiN films was thought to be disturbed by the presence of compounds of S and F with Ti on the TiN surface.
- (3) Aging treatment at 250°C for 10 h increased the EM lifetime of TiN/AlCu(0.5wt.%)/TiN/Ti multilayered lines by a factor of ten.
- (4) Segregation of Cu atoms at grain boundaries, which is invisible in standard TEM images, was detected

by EDX after aging treatment. The amount of segregated Cu reached its maximum at the aging time where EM lifetime was its maximum. Therefore, it was concluded that segregated Cu atoms invisible by TEM play an important role in improving EM resistance.

References

- 1) H. K. Kang, J. S. H. Cho, I. Asano, and S. S. Wong: "Electromigration Properties of Electroless and CVD Cu Metallization," Proceedings 9th International VLSI Multilevel Interconnection Conference, Santa Clara (USA), June (1992)
- 2) H. Hasunuma, H. Kaneko, A. Sawabe, T. Kawanoue, and Y. Kohanawa: "Single Crystal Aluminum Lines with Excellent Endurance against Stress Induced Failure," International Electron Device Meeting Technical Digest, IEEE, Washington, DC (USA), December (1989)
- 3) H. Horikoshi and T. Nogami: "Improvement EM Lifetime of AlCu/TiN Lines and W-plug Metal System by Controlling Crystal Structure of AlCu," Proceedings 10th International VLSI Multilevel Interconnection Conference, Santa Clara (USA), June (1993)
- 4) Kawasaki Steel Corp.: Jpn, Application 5-2801
- 5) T. Nemoto and T. Nogami: "Segregation of Cu to Grain Boundaries by Aging Treatment and its Effect on EM Resistance for AlCu/TiN," 31th Annual Proceedings Reliability Physics, IEEE, San Jose, April (1994)
- 6) Kawasaki Steel Corp.: Jpn, Application 5-68690
- 7) S. Vaidya and A. K. Sinha: *Thin Solid Films*, 75(1981), 253-259
- 8) K. Kageyama, K. Hashimoto and H. Onoda "Formation of Texture Controlled Aluminum and its Migration Performance in AL-Si/TiN Stacked Structure," 29th Annual Proceedings Reliability Physics, IEEE, Las Vegas (USA), April (1991)
- 9) F. M. d'Huerle, N. G. Ainslie, A. Gangulee and M. C. Shine: *J. Vac. Sci. and Technol.*, 9(1971)1, 366-372
- 10) M. Hansen: "Constitution of Binary Alloys," (1965), 84, [MacGraw-Hill, New York (USA)]
- 11) K. V. Reddy, F. Beniere, and K. Kostopoulos: *J. Appl. Phys.*, 50(1979)4, 2782-2788
- 12) D. R. Frear, J. E. Sanchez, A. D. Roming, and J. W. Morris, Jr.: *Metall. Trans. A*, 21(1990), 2449-2458
- 13) R. Rosenberg, A. F. Mayadas, and D. Gupta: *Surface Sci.*, 31(1972), 566-585